Protocol development of paired-agent fluorescent imaging to detect micrometastases in resected breast lymph nodes

Chengyue Li, Veronica C. Torres, Xiaochun Xu, Yusairah Basheer, Husain A. Sattar, et al.

Chengyue Li, Veronica C. Torres, Xiaochun Xu, Yusairah Basheer, Husain A. Sattar, Jovan G. Brankov, Kenneth M. Tichauer, "Protocol development of paired-agent fluorescent imaging to detect micrometastases in resected breast lymph nodes ," Proc. SPIE 10862, Molecular-Guided Surgery: Molecules, Devices, and Applications V, 108620U (7 March 2019); doi: 10.1117/12.2513492

SPIE.

Event: SPIE BiOS, 2019, San Francisco, California, United States

Protocol development of paired-agent fluorescent imaging to detect micrometastases in resected breast lymph nodes

Chengyue Li[1], Veronica C. Torres[1], Xiaochun Xu[1], Yusairah Basheer[1], Husain A. Sattar[2], Jovan G. Brankov[3], Kenneth M. Tichauer[1]

[1]Department of Biomedical Engineering, Illinois Institute of Technology, Chicago, IL 60616

[2]Department of Pathology, University of Chicago, Chicago, IL 60637

[3]Department of Electrical and Computer Engineering, Illinois Institute of Technology, Chicago, IL 60616

ABSTRACT

The presence of lymph node metastases played as a critical prognostic factor in breast cancer treatment and guiding the future adjuvant treatment. The possibility of missed micrometastases by conventional pathology was estimated around 20-60% cases has created a demand for the development of more accurate approaches. Here, a paired-agent imaging approach is presented that employs a control imaging agent to allow rapid, quantitative mapping of microscopic populations of tumor cells in lymph nodes to guide pathology sectioning. To test the feasibility of this approach to identify micrometastases, healthy rat and human lymph nodes were stained with targeted and control imaging agent solution to evaluate the potential for the agents to diffuse into and out of intact nodes. Erbitux, an EGFR specific antibody was labeled with IRDye-700DX(LICOR) as targeted agent and IRDye-800CW was labeled to rat IgG as control agent. Lymph nodes were stained for 60 min, followed by 30 min rinsing, and the uptake and washout of fluorescence were recorded. Subsequently, lymph nodes were frozen-sectioned and imaged under an 80-um resolution fluorescence imaging system (Pearl, LICOR) to confirm equivalence of spatial distribution of both agents in the entire node. Both imaging agents correlated well with each other($r=0.877$) and the binding potential of targeted agent was found to be 0.08 ± 0.22 along the lymph node in the absence of binding. The results demonstrate this approach's potential to enhance the sensitivity of lymph node pathology by detecting fewer than 1000 cell in a whole human lymph node.

Keywords: paired-agent fluorescent imaging, micrometastses, lymph node

1. INTRODUCTION

The status of lymph node is a key prognostic factor for staging and guiding adjuvant treatment of breast cancer[1], as the lymphatic system served as the predominant passage for tumor cell metastasis[2]. Currently, sentinel lymph node dissection is considered as a standard care of breast cancer treatment and followed by pathology examination to evaluate lymph node tumor burden[3]. However, the conventional pathology laboratories only section lymph node as 5-μm-thick slices at 2-mm intervals, as a result that less than 1% of lymph node volume was exanimated. And sections then stained with Hematoxylin and Eosin (H&E), which provides morphological information for pathologists to identify abnormal cells. It has been demonstrated that early stage metastasis disease might not be able to be detected by this routine sectioning procedure, as this method was aimed to detect tumor cells deposits greater than 2 mm in diameter, defined as macrometastases[4-6]. There is some controversy about whether detecting clusters of cells smaller than 2 mm is important[7]; however, there is growing evidence that patients with micrometastases (tumor clusters less than 2 mm in diameter) would benefit from more aggressive therapy. The estimation of undetected micrometastases using conventional method range from 20-60%[8], of which the probability increase with decreasing size of tumor.

Molecular-Guided Surgery: Molecules, Devices, and Applications V, edited by Brian W. Pogue, Sylvain Gioux,
Proc. of SPIE Vol. 10862, 108620U · © 2019 SPIE · CCC code: 1605-7422/19/$18 · doi: 10.1117/12.2513492

Numerous studies have demonstrated that micrometastases have important prognostic implication and thus more sensitive methods of detecting cancer spread to lymph node could enable earlier intervention for guiding therapeutic decision-making[9-11]. Many investigators have shown the increased ability to detect micrometastases in lymph node by taking extensive serial sectioning and immunohistochemistry[12-14]. However, these approaches are not cost-effective and too labor-intensive to be practical. Therefore, earlier and more accurate diagnostics of aggressive disease without requiring redundant time and resources is needed.

Motivated by the drawbacks of routine histology, we developed a paired-agent imaging approach by employing a control imaging agent to allow rapid, quantitative mapping of microscopic populations of tumor cells in lymph nodes to guide pathology sectioning to reduce the false negative rate. By employing paired-agent imaging strategies, recently in a metastatic mouse model demonstrated that fewer than 200 cancer-cells can be accurately detected using a wide-field non-invasive imaging of human breast cancer spread to axillary lymph nodes[15]. This proceeding was to demonstrate the development of protocol for staining *ex vivo* lymph node for further investigate the potential of paired-agent fluorescence imaging to detect micrometastases in resected breast lymph nodes.

2. METHODS AND RESULTS

2.1 Paired-agent kinetic model

The paired-agent molecular imaging estimate of targeted biomolecule concentration ("Binding Potential")[16] by employing a control imaging-agent that can essentially provides a means of correcting for the influence of tissue perfusion and non-specific uptake and retention on targeted imaging agent concentrations[17-20]. This approach assumes that the signal from the targeted imaging agent arises from concentration of imaging agent that is either bound to the specific receptor (C_b) or freely associated in the tissue (C_f). By making the assumption that the control imaging agent signal approximates the free concentration of the targeted imaging agent, the following expression can be derived:

$$\frac{Targeted - Control}{Control} \cong \frac{C_f + C_b - C_f}{C_f} = \frac{C_b}{C_f} = K_A B \equiv Binding\ Potential \quad (\mathrm{BP}),$$

where K_A is the affinity of the targeted imaging agent (a constant under most conditions) and B represents the concentration of targeted biomolecules, which for cancer-specific molecules is proportional to the number cancer cells.

For the ratiometric paired-agent imaging method to accurately estimate the binding potential or concentration of cancer cells in lymph node staining applications, both the targeted and control agents must diffuse equally to all regions of the node when the node is immersed in the solution of targeted imaging agent(s) and control imaging agent mixture in the absence of cancer cells in lymph nodes.

2.2 Evaluate paired-agent staining protocol

To evaluate the feasibility of the paired-agent imaging method to estimate the binding potential of cancer cells in resected lymph node, cancer free lymph nodes were chosen to compare kinetics with targeted and control imaging agents in the absence of binding. Lymph nodes were stained with targeted and control imaging agent solution to evaluate the potential for the agents to diffuse into and out of intact nodes. Erbitux, an EGFR specific antibody was labeled with IRDye-700DX(LICOR Biosciences) as targeted agent and IRDye-800CW was labeled to rat IgG (an isotype control of Erbitux) as control agent. Both antibodies were labeled with the NHS ester form of the fluorescent dye using manufacturer instruction.

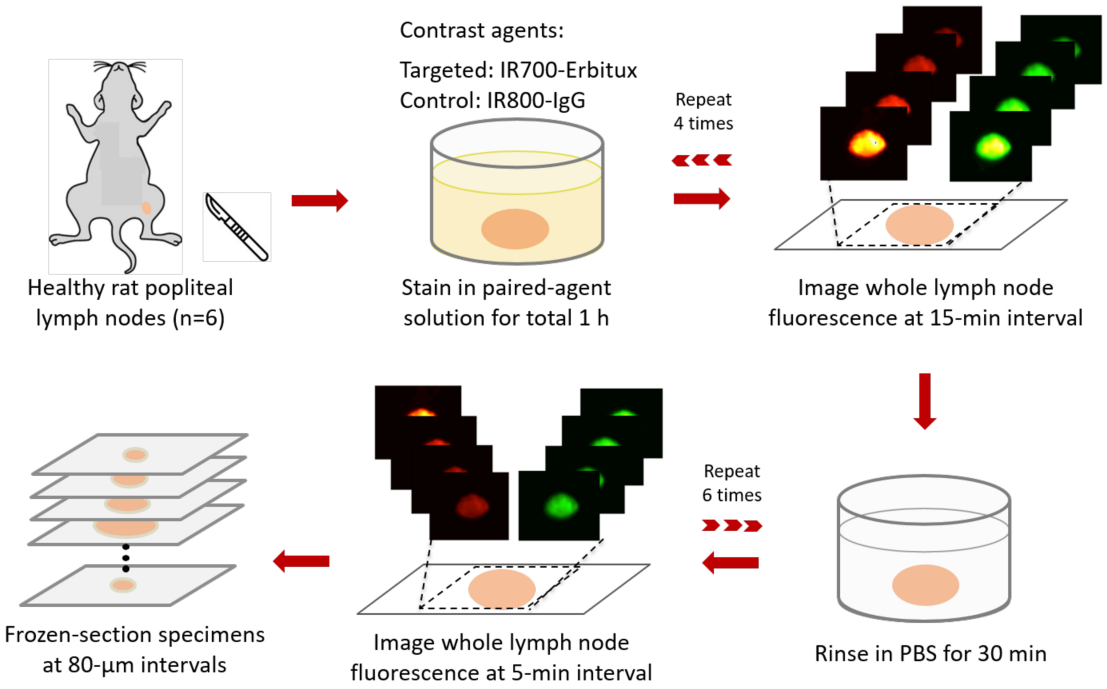

Figure 1. Stepwise illustration of rat lymph node staining and rinsing procedure.

A tissue pre-staining image was acquired to evaluate background levels caused by autofluorescence. A mixture of targeted and control imaging agent for each node was prepared at concentration of 0.1 µM IRDye700-Erbitux and 0.5 µM IRDye800-IgG. Lymph nodes were soaking in the paired-agent staining solution that covered with an aluminum foil to protect it from light at room temperature. After 15 min of staining, the lymph node was quick dip into phosphate-buffered saline (PBS) to remove excessive staining solution on the tissue surface. Whole lymph node tissue sample was immediately imaged under an 85-µm resolution fluorescence imaging system (Pearl Imager, LICOR Biosciences). Fluorescence at 700-740 nm and 800-840 nm (from 685 and 785 nm excitation, respectively) were acquired to evaluate similarity of diffusion of both targeted and control imaging agents after the staining process. Then, lymph nodes were placed back into the mixture staining solution and 4 staining time points were recorded at 15-min interval up to 1 h. Followed by rinsing in PBS and recorded every 5 min for 30 min to monitor the washout of the paired imaging agents. Autofluorescence was removed by subtracting the pre-staining image of respective imaging channels from all subsequent post-staining images. The signal intensity of the targeted and control imaging agents were compared to evaluate uptake and washout during the entire staining process.

Subsequently, lymph nodes were frozen and serial sectioned on a cryostat microtome at 80-µm intervals and the cross-sectional lymph node image of the uptake of control and targeted imaging agent were acquired on the Pearl. Spatial distributions of both imaging agents in the entire node were compared to confirm their equivalent diffusion kinetics.

2.3 Animal lymph node model

Healthy rat popliteal lymph nodes (n=6) with average size 2.29 × 1.81 mm (length × width) were used as the control lymph node mode. All animal experiments were carried out in accordance with the Institutional Animal Care and Use Committee (IACUC) at Illinois Institute of Technology under an approved protocol. All rats were fed a fluorescence free diet (Teklad global 16% protein rodent diet, 2016S, Envigo) for a week prior to imaging to reduce

tissue autofluorescence. Animals were euthanized and rat popliteal lymph nodes were excised. Lymph nodes were then stained and rinsed according to the protocol mentioned in 2.2.

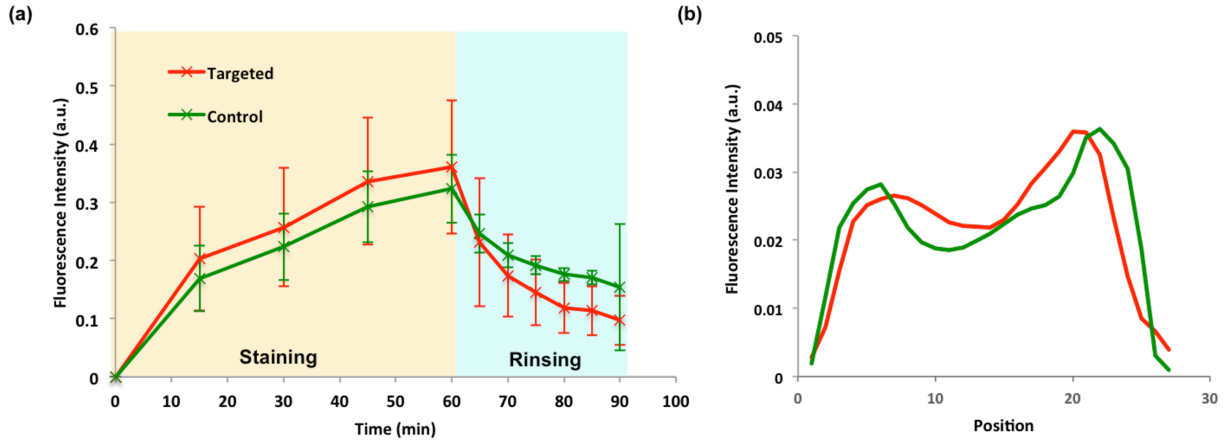

Figure 2. Paired-agent staining and rinsing protocol demonstrate in healthy rat lymph node. Rat popliteal lymph nodes were stained in mixture of target and control agent for 1 h and followed by 30 min rinsing with phosphate-buffered solution. Signal intensity of whole lymph node for targeted imaging agent (IRDye700-Erbitux) and control imaging agent (IRDye800-IgG) displayed in (a). Uptake of both imaging agent along the entire lymph node after frozen-sectioned presented in (b).

Figure 2 demonstrated that in healthy rat lymph nodes, the dynamics of uptake and washout of targeted imaging agent (IRDye700-Erbitux) is similar to control imaging agent (IRDye800-IgG) (r=0.931). Both antibody-based imaging agents are capable of penetrating the whole lymph nodes and then being washed out after the rinsing process. The uptake of both imaging agents along the cross-sectioned lymph node confirmed the comparable spatial distribution (r=0.814) and penetration into the rat lymph node.

2.4 Human lymph node model

To further test the feasibility of paired-agent fluorescent approach to clinic, human cancer free lymph nodes were isolated from fresh cadaveric tissue (n=2) were used to evaluate the protocol. Nodes were immersed in mixture agents solution and rinsed with PBS with the same protocol.

Figure 3 presented that *ex vivo* paired-agent staining and imaging of whole excised human lymph node is promising. The measured time-course average fluorescence signal of both imaging agents presented in Fig 3(a) showed a strong correlation with each other in the cancer-free lymph nodes (r=0.994, $p<0.001$). This result demonstrated the suitability of this staining and rinsing protocol with IRDye700-Erbitux as the targeted agent and IRDye800-IgG as the control agent. The equivalence of spatial distribution along the lymph node is displayed in Figure 3(b). This result demonstrated that both imaging agents correlated well with each other(r=0.877) and the binding potential of targeted agent was found to be 0.08±0.22 along the lymph node in the absence of binding, suggesting that fewer than 1000 cells may be potentially observable in a whole human lymph node.

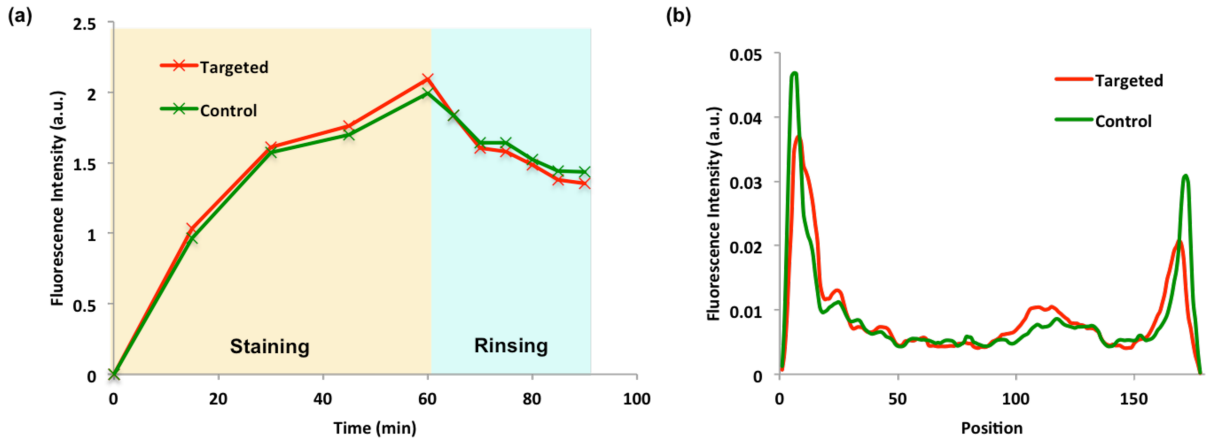

Figure 3. Paired-agent staining and rinsing protocol demonstrate in cancer free human lymph node. Healthy human lymph nodes were stained in mixture of target and control agent for 1 h and followed by 30 min rinsing with phosphate-buffered solution. Signal intensity of whole lymph node for targeted imaging agent (IRDye700-Erbitux) and control imaging agent (IRDye800-IgG) displayed in (a). Uptake of both imaging agent along the entire lymph node after frozen-sectioned presented in (b).

3. CONCLUSIONS

With equivalent distribution of both imaging agents achieved in the entire lymph node after prolonged staining and rinsing, the results demonstrate the potential of *ex vivo* paired-agent staining and imaging of whole human lymph nodes. Average wash-in and -out rates calculated here can be used in computational models to estimate the times and doses for staining and rinsing that will optimize accuracy of the paired-agent binding potential measures, determined by simulated stain and rinse protocols that yield the lowest variance in BP estimations. With 250-μm diameter cancer cells spheroid "micrometastasis" model implants into a lymph node, the paired-agent fluorescence imaging and gold standard fluorescence protein microscopy would be compared to evaluate the ability to significantly improve the sensitivity of cancer cells detection for breast cancer sentinel lymph node biopsy.

ACKNOWLEDGMENTS

The authors acknowledge support from the NSF CAREER 1653627, the Nayar Prize at IIT, and the Department of Biomedical Engineering at the Illinois Institute of Technology.

REFERENCES

[1] S. L. Chen, D. M. Iddings, R. P. Scheri *et al.*, "Lymphatic mapping and sentinel node analysis: current concepts and applications," CA Cancer J Clin, 56(5), 292-309; quiz 316-7 (2006).

[2] M. A. Swartz, and M. Skobe, "Lymphatic function, lymphangiogenesis, and cancer metastasis," Microsc Res Tech, 55(2), 92-9 (2001).

[3] G. H. Lyman, A. E. Giuliano, M. R. Somerfield *et al.*, "American Society of Clinical Oncology guideline recommendations for sentinel lymph node biopsy in early-stage breast cancer," J Clin Oncol, 23(30), 7703-20 (2005).
[4] D. L. Weaver, "Pathology evaluation of sentinel lymph nodes in breast cancer: protocol recommendations and rationale," Mod Pathol, 23 Suppl 2, S26-32 (2010).
[5] E. J. Wilkinson, L. L. Hause, R. G. Hoffman *et al.*, "Occult axillary lymph node metastases in invasive breast carcinoma: characteristics of the primary tumor and significance of the metastases," Pathol Annu, 17 Pt 2, 67-91 (1982).
[6] N. Apostolikas, C. Petraki, and N. J. Agnantis, "The reliability of histologically negative axillary lymph nodes in breast cancer. Preliminary report," Pathol Res Pract, 184(1), 35-8 (1988).
[7] P. P. Rosen, P. E. Saigo, D. W. Braun *et al.*, "Axillary micro- and macrometastases in breast cancer: prognostic significance of tumor size," Ann Surg, 194(5), 585-91 (1981).
[8] K. Tew, L. Irwig, A. Matthews *et al.*, "Meta-analysis of sentinel node imprint cytology in breast cancer," Br J Surg, 92(9), 1068-80 (2005).
[9] M. Trojani, I. de Mascarel, J. M. Coindre *et al.*, "Micrometastases to axillary lymph nodes from invasive lobular carcinoma of breast: detection by immunohistochemistry and prognostic significance," Br J Cancer, 56(6), 838-9 (1987).
[10] "Prognostic importance of occult axillary lymph node micrometastases from breast cancers. International (Ludwig) Breast Cancer Study Group," Lancet, 335(8705), 1565-8 (1990).
[11] P. J. Hainsworth, J. J. Tjandra, R. G. Stillwell *et al.*, "Detection and significance of occult metastases in node-negative breast cancer," Br J Surg, 80(4), 459-63 (1993).
[12] S. Friedman, F. Bertin, H. Mouriesse *et al.*, "Importance of tumor cells in axillary node sinus margins ('clandestine' metastases) discovered by serial sectioning in operable breast carcinoma," Acta Oncol, 27(5), 483-7 (1988).
[13] P. Ambrosch, and U. Brinck, "Detection of nodal micrometastases in head and neck cancer by serial sectioning and immunostaining," Oncology (Williston Park), 10(8), 1221-6; discussion 1226, 1229 (1996).
[14] R. J. Cote, H. F. Peterson, B. Chaiwun *et al.*, "Role of immunohistochemical detection of lymph-node metastases in management of breast cancer. International Breast Cancer Study Group," Lancet, 354(9182), 896-900 (1999).
[15] K. M. Tichauer, K. S. Samkoe, J. R. Gunn *et al.*, "Microscopic lymph node tumor burden quantified by macroscopic dual-tracer molecular imaging," Nat Med, 20(11), 1348-53 (2014).
[16] M. A. Mintun, M. E. Raichle, M. R. Kilbourn *et al.*, "A quantitative model for the in vivo assessment of drug binding sites with positron emission tomography," Ann Neurol, 15(3), 217-27 (1984).
[17] K. M. Tichauer, Y. Wang, B. W. Pogue *et al.*, "Quantitative in vivo cell-surface receptor imaging in oncology: kinetic modeling and paired-agent principles from nuclear medicine and optical imaging," Phys Med Biol, 60(14), R239-69 (2015).
[18] K. M. Tichauer, K. S. Samkoe, W. S. Klubben *et al.*, "Advantages of a dual-tracer model over reference tissue models for binding potential measurement in tumors," Phys Med Biol, 57(20), 6647-59 (2012).
[19] C. Li, V. C. Torres, and K. M. Tichauer, "Noninvasive detection of cancer spread to lymph nodes: A review of molecular imaging principles and protocols," J Surg Oncol, 118(2), 301-314 (2018).
[20] C. Li, X. Xu, N. McMahon *et al.*, "Paired-Agent Fluorescence Molecular Imaging of Sentinel Lymph Nodes Using Indocyanine Green as a Control Agent for Antibody-Based Targeted Agents," Contrast Media & Molecular Imaging, 2019, 13 (2019).